New Solutions on the Design of a Galileo Acquisition-Aiding Signal to Improve the TTFF and the Sensitivity

Lorenzo Ortega Espluga, *TéSA*
Charly Poulliat, Marie-Laure Boucheret, *ENSEEIHT*
Marion Aubault, *CNES*
Hanaa Al Bitar, *Thales Alenia Space*

BIOGRAPHIES

Lorenzo Ortega Espluga received the Eng. degree in Telecommunication Engineering in 2014, and the M.Sc degree in Telecommunication and Signal Processing in 2016, both from Zaragoza University. In 2016, he coursed the Second year of International Master of Electronics Systems for Embedded and Communicating Applications at the INP-ENSEEIHT (University of Toulouse) as an exchange Student. Currently he is a PhD Student at ENSEEIHT and studies methodologies to optimize the signal structure of the new generation of Galileo. His thesis is funded by CNES (French Space Agency) and Thales Alenia Space.

Charly Poulliat received the Eng. degree in Electrical Engineering from ENSEA, Cergy-Pontoise, France, and the M.Sc. degree in Signal and Image Processing from the University of Cergy-Pontoise, both in June 2001. From Sept. 2001 to October 2004, he was a PhD student at ENSEA/University Of Cergy-Pontoise/CNRS and received the Ph.D. degree in Signal Processing for Digital Communications from the University of Cergy-Pontoise. From 2004 to 2005, he was a post-doctoral researcher at UH coding group, University of Hawaii at Manoa. In 2005, he joined the Signal and Telecommunications department of the engineering school ENSEA as an Assistant Professor. He obtained the habilitation degree (HDR) from the University of Cergy-Pontoise in 2010. Since Sept. 2011, he has been a full Professor with the National Polytechnic Institute of Toulouse (University of Toulouse, INP-ENSEEIHT). His research interests are signal processing for digital communications, error control coding and resource allocation.

Marie-Laure Boucheret received the Eng. degree in Electrical Engineering from ENST Bretagne, Toulouse, France, and the M.Sc. degree in Signal Processing from the University of Rennes, both in June 1985. In june 1997, she received the Ph.D. degree in Communications from TELECOM ParisTech, and the "Habilitation à diriger les recherches" in June 1999 from INPT University of Toulouse. From 1985 to 1986 she has been a research engineer at the French Philips Research Laboratory (LEP). From 1986 to 1991, sha has been an engineer at Thales Alenia Space, first as a project Engineer (TELECOM II program) then as a study engineer at the transmission laboratory. From 1991 to 205 she was a Associated professor then a Professor at TELECOM ParisTech. Since March 2005 Marie-Laure Boucheret is a Professor at the National Polytechnic Institute of Toulouse (ENSEEIHT - University of Toulouse). She is also with the Signal and Communication group of the IRIT Laboratory.

Marion Aubault-Roudier is a radionavigation engineer in the navigation/location signals department in CNES, the French Space Agency, where she is involved in the optimization of GNSS signals as well as the assessment of GNSS user segments (receivers, algorithms). Marion Aubault-Roudier graduated as an electronics engineer in 2011 from ENAC (Ecole Nationale de l'Aviation Civile) in Toulouse, France. She received her PhD in 2015 from the Department of Mathematics, Computer Science and Telecommunications of the INPT (Polytechnic National Institute of Toulouse), France.

Hanaa Al Bitar is a GNSS systems engineer at Thales Alenia Space France. She received her Ph.D in RadioNavigation in 2007 form the ENAC, in Toulouse, France, in the field of GNSS Receivers. She joined TAS-F in 2012. Her main activities focus on GNSS signal processing, and SBAS Land Earth Stations signal processing and design.

ABSTRACT
The design of a new GNSS signal is always a trade-off between improving performance and increasing complexity, or even between improving different performance criteria. Position accuracy, receiver sensitivity (acquisition, tracking or data demodulation thresholds) or the Time-To-First-Fix (TTFF) are examples of those GNSS receivers performance criteria. Within the framework of Galileo 2nd Generation (G2G), adding a new signal component dedicated to aid the acquisition process on E1 can help to improve performance of GNSS receivers with respect to these criteria as it was shown in [1]. In order to create this new component, various aspects such as the spreading modulation, the data navigation content, the channel coding or the Pseudo-Random Noise (PRN) codes must be studied. To this end, this paper firstly proposes the study of new spreading modulations, and secondly, we investigate on PRN codes that can be well suited to the proposed Acquisition-Aiding signal.

INTRODUCTION
In the current framework of Galileo, a new Acquisition-Aiding signal can help to improve the acquisition and sensitivity of the GNSS receiver. Several aspects must be taken under consideration in order to design a new signal component, such as the spreading modulation, the data navigation content, the channel coding, the Pseudo-Random Noise (PRN) codes or the method to multiplex such a signal with the existing signals components. In this paper, firstly we focus on the search for new spreading modulations which provide robustness during the acquisition stage for the new Acquisition-Aiding signal, and secondly, we investigate on well suited spreading codes which reduce the degradation on the acquisition and tracking stages under hostile environments.

Concerning the definition of a new spreading modulation, a fundamental criterion is the Radio Frequency Compatibility (RFC) [2], since backward-compatibility between new and current signals is crucial. Other decisive parameters such as the correlation properties, the jamming or the robustness against distortions due to the multipath are evaluated.
In this paper, we propose the family of Binary Code Symbols (BCS) spreading modulations [4] as new spreading modulation candidates for the Acquisition-Aiding signal component. We compare such candidates with the current state of the art (Binary Offset Carrier (BOC) modulation [5] and Binary Phase Shift Keying (BPSK) [1]. Performance criteria such as the autocorrelation function (first to secondary peak-to-peak ratio), the Spectral Separation Coefficients (SSC), the Gabor bandwidth, the MultiPath Error Envelope (MPEE) or the anti-jamming coefficients are evaluated. In addition, a 4 MHz shifted BPSK(1) is assessed.

Concerning the search for new PRN codes, to generate a subset of chip spreading codes, several methodologies have been proposed so far and a simple model criterion based on a weighted cost function [3] is used to evaluate the spreading codes performance. According to [3], the cost function is a weighted compound objective function taking into account different properties such as the autocorrelation, the cross-correlation and the power spectral density. In this context, three families of 1023 chips are investigated in this paper as new PRN candidates for the new Acquisition-Aiding signal component: a Gold code family, a large Kasami code family and an optimized random code family, based on the current E1-B PRN codes generation technique [6].

The paper is organized as follows. Section I introduces the spreading modulation criteria as well as the mathematical tools to compare those criteria. Section II introduces the family of BCS spreading modulations and compares the specific BCS [-1, -1, -1, 1, -1] (1) with the candidates of the current state of the art (BOC modulation and BPSK). Section III describes the spreading code selection criteria as well as the mathematical tools to compare the codes. Section IV presents the spreading codes families as well as the method to generate each family and shows the spreading code families results. Conclusions are finally drawn in Section V.

I - SPREADING MODULATION CRITERIA
Concerning the design of a new Acquisition-Aiding signal, various criteria (listed in table 1) must be studied in order to select the spreading modulation.

A first fundamental criterion is the **RFC** [2], to ensure the backward-compatibility between new and current signals. In order to select some of the spreading modulations, as it was proposed in [1], a criterion of “acceptability” based on the degree of interference between signals is defined. Such a degree of interference represents the spectral overlap between signals and is computed by SSCs [1] [2].

In terms of **correlation properties**, in addition to the Auto-Correlation Function (ACF), another important criterion can be defined. Keeping in mind that the new component is aimed to be an Acquisition-Aiding signal, it is crucial that the ACF first to secondary peak-to-peak ratio will be as high as possible in order to ease the acquisition process, since high secondary peaks increment the acquisition error probability.

In order to quantize the **resistant against multipath**, the distortions caused by the multipath have to be evaluated over the spreading modulation candidates. These distortions directly affect the correlation properties of the signal and have a direct consequence to the discrimination function used on the receiver. In order to evaluate such as distortion, the MPEE [9] [17] [18], which quantizes the bias error induced by the multipath, is computed.

The **ranging performance** is evaluated by the theoretical accuracy of the time-delay estimation, which can be represented by the Gabor bandwidth [10] considered as an alternative interpretation of the Cramér-Rao lower bound [10]. Therefore the greater the Gabor bandwidth is, the better the performance in terms of code-tracking accuracy.

The **anti-jamming capability** is predicted based on four parameters [16] [17] [18] based on the effective carrier to noise density ratio $(C/N0)eff$ [2], which indicates the level of interference at the input of the receiver. Higher anti-jamming coefficients involve less vulnerability to the jamming attacks.

Figures of Merit	Criteria	Equations	Unknowns
RFC	SSC	$K_{ss} = \int_{-Br/2}^{Br/2} G^2{}_s(f)df$ [2] (1) $K_{si} = \int_{-B/2}^{B/2} G_s(f)G_i(f)df$ [2] (2)	K_{ss} SSC of the desired signal K_{si} SSC between the desired signal and the interfering signal $G_s(f), G_i(f)$ normalized PSDs of the desired and interfering signals Br front-end bandwidth PSD Power Spectral Density of the desired signal ε code delay estimation error a multipath signal to direct signal amplitude ratio d correlator spacing R_d data rate τ time delay
Correlation Properties	ACF	$ACF = \int_{-Br/2}^{Br/2} PSD * e^{j\omega t}\, df$ [7] (3)	
Resistance Against Multipath	MPEE	$\varepsilon \approx \frac{\pm a \int_{-\frac{Br}{2}}^{\frac{Br}{2}} G_s(f)\sin(2\pi f\tau)\sin(2\pi f d)\, df}{2\pi \int_{-\frac{Br}{2}}^{\frac{Br}{2}} G_s(f)\sin(2\pi f d)\,[1 \pm a\cos(2\pi f\tau)]df}$ [9] (4)	
Ranging Performance	Gabor bandwidth	$f_{Gabor} = \sqrt{\int_{-Br/2}^{Br/2} f^2 G_s(f)\, df}$ [10] (5)	
Anti-Jamming Capability	Demodulation & anti-jamming of narrowband	$Q_{\text{Dem\&AJNB}} = 10log_{10}\left(\frac{1}{R_d * \max(G_s(f))}\right)\, dB$ [18] (6)	
	Code Tracking & anti-jamming of narrowband	$Q_{\text{CT\&AJNB}} = 10log_{10}\left(\frac{\int_{-Br/2}^{Br/2} f^2 G_s(f)\, df}{\max(f^2 G_s(f))}\right)\, dB$ [18] (7)	
	Demodulation & anti-jamming of matched spectrum	$Q_{\text{Dem\&AJMS}} = 10log_{10}\left(\frac{1}{R_d \int_{-Br/2}^{Br/2} {G_s}^2(f)\, df}\right)\, dB$ [18] (8)	
	Code Tracking & anti-jamming of matched spectrum	$Q_{\text{CT\&AJMS}} = 10log_{10}\left(\frac{\int_{-Br/2}^{Br/2} f^2 G_s(f)\, df}{\int_{-Br/2}^{Br/2} f^2 {G_s}^2(f)\, df}\right)\, dB$ [18] (9)	

Table 1 Spreading Modulation Selection Criteria

II BCS AS A NEW SPREADING MODULATION CANDIDATE

Definition of BCS Modulation

The Binary Code Symbols modulation was shown to be a generalization of the BPSK with rectangular symbols and BOC modulations [4]. Indeed the well-known BPSK and BOC_{cos} modulations, which are used as current GNSS modulations, can be shown as a particular case of the BCS modulation.

Following [4], the signal model for a spread spectrum sequence is represented as:

$$s(t) = \sum_{k=-\infty}^{\infty} a_k q(t - kT_c) \tag{10}$$

where a_k represents a sequence of spreading values which modify the spreading symbol $q(t)$ and T_c is the chip interval duration for each spreading symbol. One of the constraints for any GNSS system is that the emitted signal must have a constant envelope in order to avoid signal distortions at the output of the power amplifier. As a consequence the values of $a_k \in \mp 1$ and $q(t)$ must be a constant real value.

For the case of the BCS modulation, it can be considered that each spreading symbol is modulated by a fixed sequence of K values. Each value is considered as a segment of length equal to T_c/K. As a consequence the new spreading symbol can be represented as:

$$q(t) = \sum_{k=0}^{K-1} c_k p(t - kT_c/K) \tag{11}$$

where $p(t)$ is 1 inside the spreading symbol period and 0 otherwise. Following [4], BCS $([c_0, c_1, c_2 \ldots, c_{K-1}], f_c)$ is the notation used to denote a BCS modulation that uses the specific sequence $[c_0, c_1, c_2 \ldots, c_{K-1}]$ and f_c denotes the spreading symbol rate. In Figure 1, it is illustrated a graphic example of how to generate the BCS$([0,1,0,1,0,1,1,1], f_c)$ spreading modulation. In this example $K = 8$ and as a consequence each value has a period of $T_c/8$.

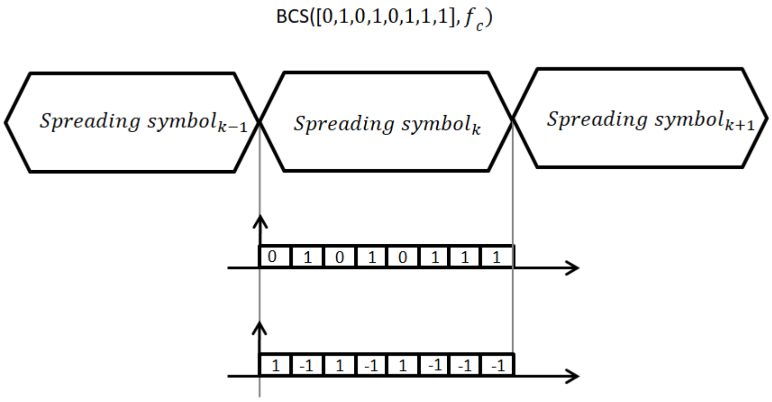

Figure 1 BCS Chip Waveform

Selection of the Best Spreading Modulation Candidate for the New Acquisition–Aiding Signal

In order to select the best spreading modulation candidate, first we define the spectra of the current CDMA GNSS systems [1] working at the band E1/L1/B1 (Table 2 and Figure 2).

GNSS System	Galileo	Compass	GPS
Signal	E1-OS and E1-PRS	B1-AS and OS	M-Code, P(Y), L1 C/A and L1C
Spreading modulation	MBOC and BOCcos(14,2)	BOCcos(14,2),TMBOC	BOCsin(10,5),BPSK(10), BPSK(1) and TMBOC

Table 2 Existing Signals and Spreading Modulations

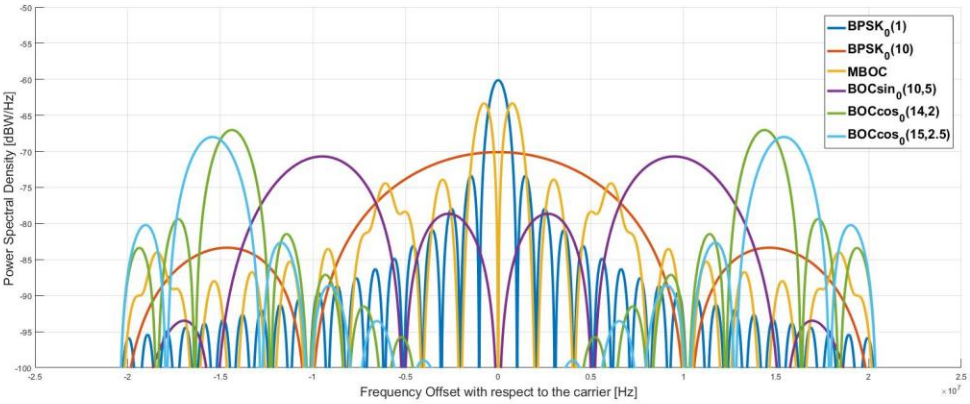

Figure 2 GNSS/E1/L1/B1 Signals PSD

RFC

The SSC (1) and (2) of the signal candidates are evaluated and illustrated in Figure 3. Those spreading modulations must satisfy the acceptability criterion, otherwise, in case of having high SSCs, they will be dropped.

It must be pointed out that BOC spreading modulation candidates were already proposed as possible candidates in [1]. Table 3 illustrates the proposed candidates.

Already Proposed Candidates	Proposed Candidates
BOCsin(6.5,0.5)	BCS[-1,1](0.5)
BOCcos(6.5,0.5)	BCS[-1,1,-1](0.5)
BOCsin(4,0.5)	BCS[-1,-1,-1,1,1](0.5)
BOCcos(4,0.5)	BCS[-1,-1, -1, 1, 1](1)
BOCsin(4, 1)	BCS[-1,1,-1](1)
BOCcos(4,1)	BCS[-1,-1,-1,1,-1](1)
BOCcos(0.5,0.5)	
BOCsin(0.5,0.5)	

Table 3 Evaluated Spreading Modulation Candidates

Figure 3 shows that BOCsin(0.5,0.5), BCS[-1 1](0.5) , and BCS[-1 -1 -1 1 1](0.5) spreading modulations are discarded due to the interference caused on the BPSK spreading modulation used by the GPS C/A signal: $BPSK_0(1)$. Finally, Table 4 illustrates the suitable candidates once the RFC criterion has been assessed.

Suitable Candidates	
BOCsin(6.5,0.5)	BCS[-1,1,-1](0.5)
BOCcos(6.5,0.5)	BCS[-1,-1, -1, 1, 1](1)
BOCsin(4,0.5)	BCS[-1,1,-1](1)
BOCcos(4,0.5)	BCS[-1,-1,-1,1,-1](1)
BOCsin(4, 1)	
BOCcos(4,1)	
BOCcos(0.5,0.5)	

Table 4 Suitable Spreading Modulation Candidates After RFC Criterion

SSC Coefficients

	BPSK$_0$(1)	BPSK$_0$(10)	MBOC	BOCsin$_0$(10,5)	BOCcos$_0$(14,2)	BOCcos$_0$(15,2.5)
BOCcos$_0$(6.5,0.5)	-88.43	-78.27	-79.09	-77.49	-90.91	-90.29
BOCsin$_0$(6.5,0.5)	-85.40	-77.79	-78.46	-77.85	-94.23	-92.64
BOCcos$_0$(4,0.5)	-88.96	-73.54	-87.47	-80.91	-96.51	-94.08
BOCsin$_0$(4,0.5)	-82.93	-73.26	-82.99	-81.20	-95.06	-94.09
BOCcos$_0$(4,1)	-85.95	-73.66	-84.46	-80.46	-93.48	-93.83
BOCsin$_0$(4,1)	-79.92	-73.11	-79.98	-81.00	-92.04	-93.84
BOCcos$_0$(0.5,0.5)	-66.12	-70.48	-65.27	-83.92	-92.96	-93.57
BOCsin$_0$(0.5,0.5)	-63.11	-70.32	-66.52	-86.13	-95.17	-95.79
BCS[-1 1](0.5)	-63.11	-70.32	-66.52	-86.13	-95.17	-95.79
BCS[-1 1 -1](0.5)	-66.75	-70.48	-64.86	-83.92	-92.94	-93.56
BCS[-1 -1 -1 1 1](0.5)	-63.09	-70.32	-66.57	-86.13	-95.17	-95.79
BCS[-1 -1 -1 1 1](1)	-67.39	-70.56	-65.50	-83.12	-91.68	-92.80
BCS[-1 1 -1](1)	-71.40	-70.89	-68.98	-80.90	-88.80	-91.90
BCS[-1 -1 -1 1 -1](1)	-66.11	-70.89	-69.37	-80.90	-91.31	-94.60

More interference ← Less interference

Figure 3 SSC Coefficients Between Legacies and Proposed Signals

Correlation Properties

A very low first to secondary peak to peak ratio on the autocorrelation function increases the false lock error probability and it induces problems at the acquisition stage. In figure 4, the normalized autocorrelation function for each spreading modulation candidate is illustrated; those with a high secondary peak have been discarded: BOCsin(4,0.5), BOCcos(4,0.5), BOCsin(4,1), BOCcos(4,1), BOCsin(6.5,0.5) and BOCcos(6.5,0.5).

It is worth stressing the BCS[-1 -1 -1 1 -1](1) spreading modulation, whose low secondary autocorrelation peak clearly outperforms the remaining candidates. Moreover, such a spreading modulation has a small width on the main autocorrelation peak which involves better ranging precision. For such a property, BCS[-1 -1 -1 1 -1](1) and BCS[-1 1 -1](1) outperform the other candidates.

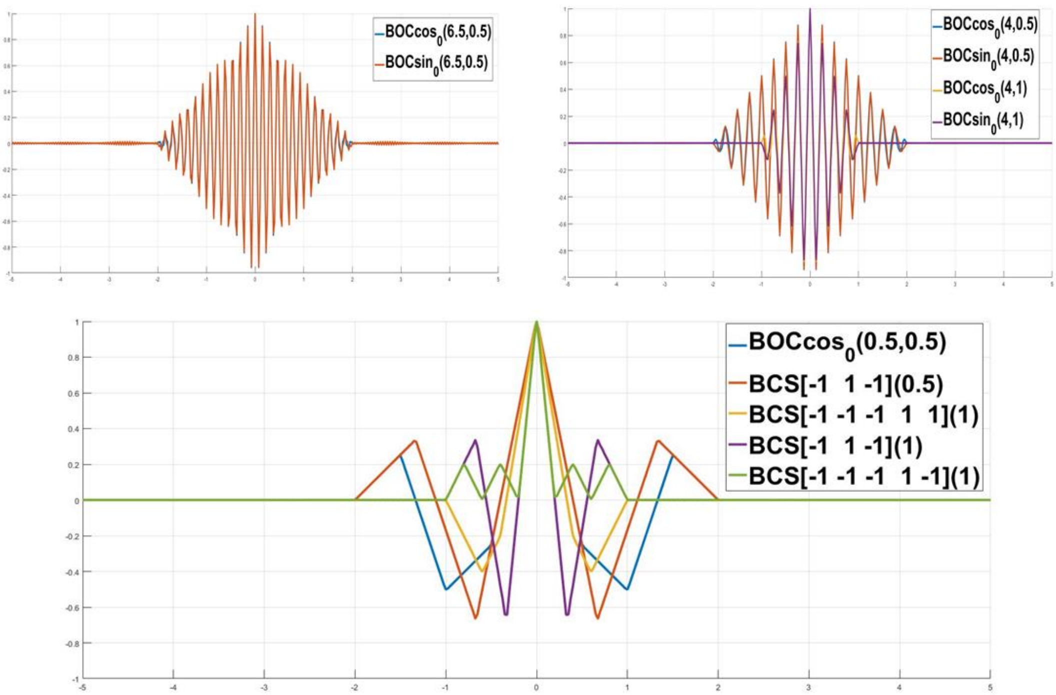

Figure 4 ASF Candidate Signals

Resistance Against Multipath

In order to obtain the MPEE results, a front-end bandwidth of 40 MHz, an early-late correlator with a chip spacing $d = 0.1$ chips and a multipath signal to direct signal amplitude ratio $a = 0.1$ have been selected. MPEE [17] [18] has been obtained for both cases, the extreme case $\Delta\phi = 0°$, where the direct signal and the multipath signal are in phase and with $\Delta\phi = 180°$, where signal and multipath are in contra-phase. Following equation (4), it is expected that solutions with lowest chip rate and subcarrier-frequency result in worst resistance to multipath. Indeed, BOCcos(0.5, 0.5) and BCS[-1 1 -1](0.5) spreading modulations show the poorer performance in terms of MPEE. On the other hand, the sharpest autocorrelation peak of the BCS[-1 -1 -1 1 -1](1) spreading modulation provides the best results with lower multipath error as a function of the multipath delay.

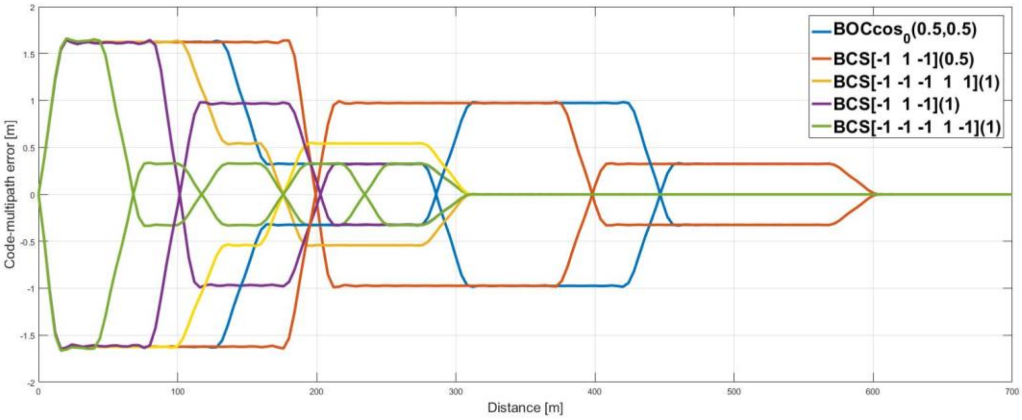

Figure 5 MPEE Candidate Signals

Ranging Performances

Following equation (5), the Gabor bandwidth is computed as a function of the front-end bandwidth for a range from 2 to 40 MHz. In terms of performance, the greater bandwidth, the better code-tracking accuracy is obtained. BCS[-1 -1 -1 1 -1](1) and BCS[-1 1 -1](1) obtain the greater ranging performance as of 4 MHz. However, for a front-end bandwidth of 2 MHz, BOCcos(0.5, 0.5) and BCS[-1 1 -1](0.5) obtain the higher Gabor bandwidth because most of the power of such spreading modulation is concentrated through 1 MHz.

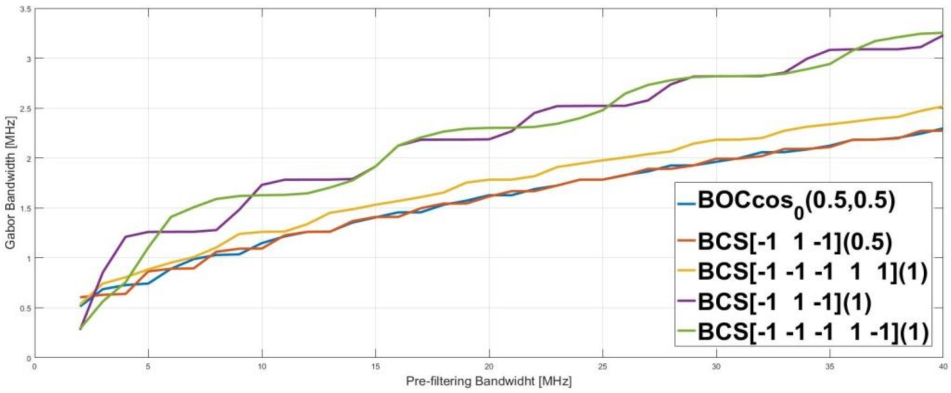

Figure 6 Gabor Bandwidth Candidate Signals

Anti-Jamming Capability

The anti-jamming coefficients for a front-end bandwidth of 40 MHz are illustrated in Figure 7. Clearly, BCS[-1 -1 -1 1 -1](1) presents a superior Dem&AJNB and Dem&AJSM performance among the signals due to its flatter power distribution. Concerning CT&AJNB and CT&AJMS coefficients, candidates do not show differences bigger than 3 dB.

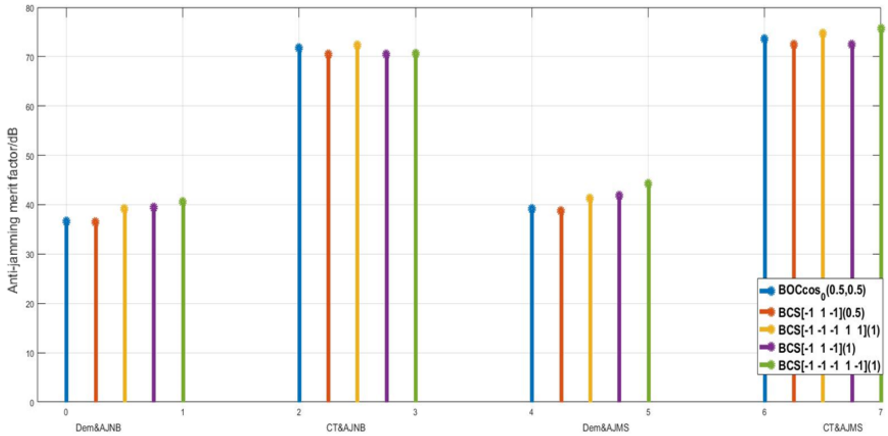

Figure 7 Anti-Jamming Coefficients Front-End Bandwidth of 40 MHz

Summing up this evaluation, it seems that the most interesting solution for the new Acquisition-Aiding signal is the BCS[-1 -1 -1 1 -1](1) spreading modulation. Spectrum of the final candidate along with the current signals is illustrated in Figure 8. The wide power spectrum density of BCS[-1 -1 -1 1 -1](1) (almost 6 MHz) is remarkable, which provides good anti-jamming and multipath rejection performance. On the other hand, the use of small front-end bandwidth at the receiver leads to degradations in the ranging performance, since most of the useful signal has been filtered by this front-end filter.

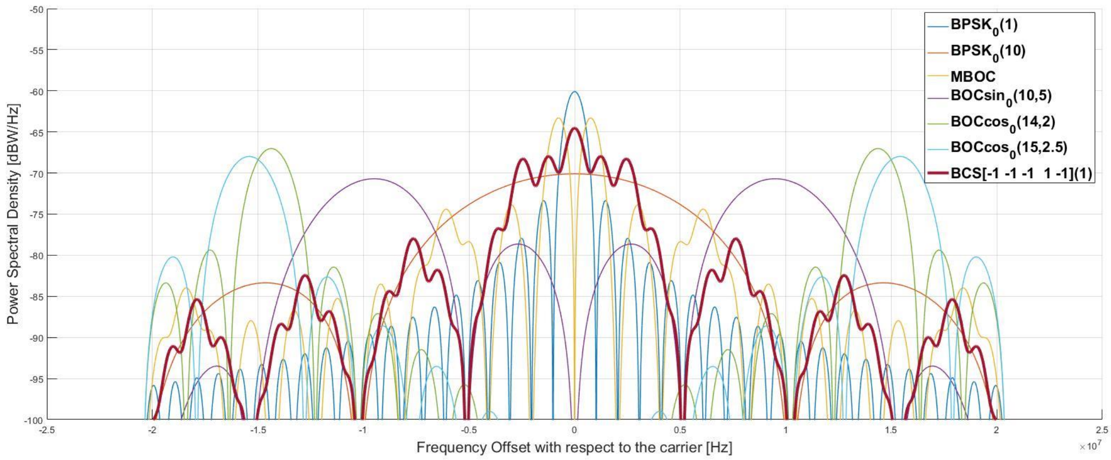

Figure 8 Spectrum of BCS[-1 -1 -1 1 -1](1) Along With Legacy Signals

Introduce a Shifted BPSK as a Possible Candidate

As it is well known, a very low first to secondary peak to peak ratio within the autocorrelation function will increase the false lock probability error on the acquisition stage. Moreover, for the BPSK spreading modulation, which is used in the GPS L1 C/A signal [8], there are no ACF secondary lobes. The following proposition is based on both previous concepts and consists in using a shifted BPSK spreading modulation as a candidate for the new Acquisition-Aiding signal.

Two shifted BPSK spreading modulations are evaluated, where the central frequency is $f_{L1} + f_i$ with $f_i \in \{3f_0, 4f_0\}$ and f_0 is the chip frequency used in the GPS L1 C/A signal.

Figure 9 illustrates the BPSK performance and compares it with the BCS candidate performance proposed before. The autocorrelation function shows the absence of secondary side lobe within the autocorrelation function, which provides a better resilience to false lock probability. Moreover the SSCs show a higher isolation between the candidates and the current signals. By the other hand, as the BPSK spreading modulation has smaller bandwidth, the MPEE and the anti-jamming coefficients show worst performance than the BCS[-1 -1 -1 1 -1](1) spreading modulation. Concerning the Gabor bandwidth, BCS[-1 -1 -1 1 -1](1) shows better performance until 6 MHz, since the power spectral density is not shifted. Finally, it must be remarked that shifting the spreading modulation involves an increase of the receiver complexity either due to the increase of the front-end bandwidth or to not operate in the central frequency of E1 band.

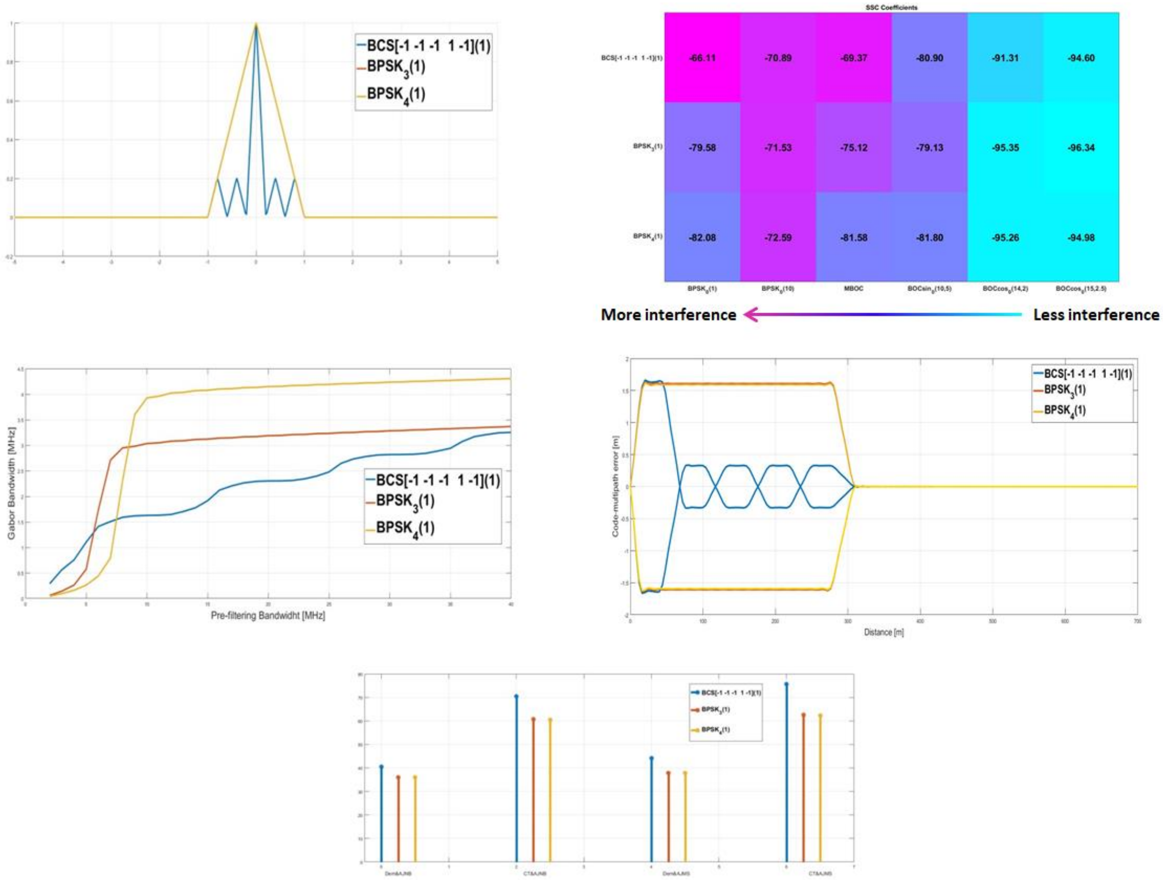

Figure 9 BPSK Criteria Performances

III SPREADING CODES CRITERIA FOR THE NEW ACQUISTION-AIDING SIGNAL

In this section, in order to select the best chip spreading codes, a weighted cost function will be evaluated according to a set of criteria [3], based on the autocorrelation and cross-correlation functions. In theory, an ideal spreading code is orthogonal with any of its delayed versions and with the entire family codes. This involves that the autocorrelation function is null for any relative non-null chip delay and the cross-correlation is null for any relative delay value. Of course, ideal spreading codes are not achievable. The currently used imperfect spreading codes obviously underperform with respect to a hypothetical ideal code, and this has an impact on the receiver final performance. Following [3], three different criteria have been implemented (listed in table 5). Those criteria represent the effect of the non-ideal spreading codes over the acquisition and tracking processes as well as over the robustness against narrow-band interferences. All the theoretical background of the cross-correlation is described in [11].

The **acquisition criterion** aims for detecting unwanted correlation peaks at the acquisition process. Those correlation peaks arise under hostile environments, where huge attenuations or strong multipath affect the correlation properties of the signal itself and degrade the cross-correlation properties in presence of other Galileo satellites signals. An increase of the secondary correlation peak leads to an increase of the false acquisition probability, which induces a reduction of the detection performance. A simple mathematical model [3] based on the Welch bound [11] is considered to quantify these effects. The Mean Excess Welch Square Distances $MEWD^{MP}$ (13) criterion is used to evaluate the effects of the multipath on the desired signal and is mainly based on the analysis of the ACF function. The Mean Excess Welch Square Distances ${MEWD_{i,j}}^{CT}$ (14) criterion is used to evaluate the effect of the Galileo navigation (intra-system) signals from other satellites on the direct path. In order to evaluate the impact over all the code family, average values of $MEWD^{MP}$ and ${MEWD_{i,j}}^{CT}$ are computed.

In the tracking mode, the whole correlation function quality must be taken into account in order to assess the receiver final tracking performance. Indeed, as it was shown in [12], any non-ideal spreading code introduces an aggregate perturbation denominated *average interference parameter,* which directly affects the average signal to noise ratio in the receiver. In order to evaluate such effects, a **tracking criterion** called Merit Factor MF_i^{MP} (14), which evaluates the multipath effect onto the tracking mode and a tracking criterion called Merit Factor $MF_{i,j}^{CT}$ (15), which evaluates the effect of the non-desired satellite signals are presented. Average values are computed in order to evaluate the effect over all the code family.

Considering a hypothetical situation where the navigation signal is generated by an ideal spreading code (infinite period), the power spectral density should match with the exact envelope shape of the spreading modulation. However, under real conditions (finite spreading codes) the lack of pure sequences shows peaks exceeding this envelop. Accordingly, the receiver sensitivity to continuous wave interference is increased.

A spreading code with good **robustness against narrowband interfering signals** should have as less peaks which exceed the ideal PSD for the pulse shape envelop as possible. In order to assess such a property, the Excess Line Weight (ELW) is defined (16). Average values are computed in order to evaluate the effect over all the code family.

A single relative weighted cost function can be used to handle an unambiguous methodology to evaluate and compare the code sets. The relative weighted cost function is defined in (17).

$$R_i = \sum_{j=1}^{5} -w_j \frac{\overline{cv_j} + cv_{i,j}}{\overline{cv_j}} \; for\ i = 1,2, \dots K \tag{17}$$

where $\overline{cv_j}$ is the mean value of the criterion j over all different code sets, $cv_{i,j}$ is the value of criterion j and code set i and w_j is the weighting factor of criterion j. Depending on the final use of the signal, the weighted values depend of the degree of importance between the different criteria. For instance, in the new Acquisition-Aiding signal generation, the acquisition criterion should be emphasized.

Criteria	Equations	Unknowns
Acquisition Criterion	$MEWSD^{MP} = mean\left(\sum_{n_{foffs}} \sum_{\substack{l=1 \\ ACF^e(l,f_{offs})>\Phi_{min}}}^{N-1} (ACF^e(l,f_{offs}) - \Phi_{min})^2\right)$ [3] (12) $MEWSD^{CT}{}_{i,j} = mean\left(\sum_{n_{foffs}} \sum_{\substack{l=1 \\ CC^e(l,f_{offs})>\Phi_{min}}}^{N-1} (CC^e(l,f_{offs}) - \Phi_{min})^2\right)$ [3] (13)	Φ_{min} Welch Bound f_{offs} frequency offsets ACF^e even ACF CC^e even cross-correlation function n_{foffs} number of frequency offsets A_k k^{th} value of the discrete Fourier transform n number of frequency points
Tracking Criterion	$MF_i^{MP} = \frac{1}{n_{foffs}}(\sum_{n_{foffs}}(\sum_{l=1,2,N-2,N-1}(ACF_i^e(l,f_{offs}))^2)$ [3] (14) $MF_{i,j}^{CT} = \frac{1}{n_{foffs}}(\sum_{n_{foffs}}(\sum_{l=0}^{N-1}(CC_{i,j}^e(l,f_{offs}))^2)$ [3] (15)	
Robustness Against Narrow-Band Interferences Criterion	$ELW = 10\log(\frac{1}{n}\sum_{\substack{k=-\frac{n}{2} \\ A_k>\sqrt{n}}}^{\frac{n}{2}}(A_k - \sqrt{n})^2)$ [3] (16)	

Table 5 Spreading Codes Criteria

IV CONSTRUCTION OF THE FAMILY CODES

Section IV explains the design and construction of several families of spreading codes, which will be proposed as possible candidates for the new Acquisition-Aiding Signal. One of the most remarkable constraints on the design of a new spreading code family is the length of the code which shall be as short as possible, since the new component shall allow a faster acquisition process. We propose a 1023 chips code length, since it is the smallest length which is an entire divisor of the chip frequency 1.023MHz and can be generated by a mathematical method.

In [13], several mathematical spreading codes families with a 1023 chips length are illustrated. Some of them, like the Gold codes family, have been already used in the design of GNSS signals [8]. Other families such as large Kasami codes could potentially be suitable spreading codes family candidates. Other methodologies have been proposed in [6] to generate efficient memory codes; these methodologies apply a cost function with constraints in order to optimize some properties or criteria. In this paper we are going to develop three spreading code families, the first two families are a Gold and a large Kasami spreading code families and the third family applies the methodology describes in [6] in order to generate a memory code with length 1023 chips.

Gold Codes

Gold codes are one important class of periodic sequences, which provides reasonably large sets of codes with good periodic cross-correlation and autocorrelation properties. Gold codes have a code period of $N = 2^n - 1$ chips and have N+2 codes in the set. These codes are constructed from selected m-sequences [14] and particularly by a *preferred pairs of m-sequences* [14] of length N. Following Theorem 2 [14], a *preferred pairs of m-sequences a* and *b* of period $N = 2^n - 1$ generated by primitive binary polynomials with no common factor and where $\neq 0\, mod\, 4$ is defined. The set of sequences defined by $G(a, b)$ is called Gold codes.

$$G(a, b) = \{a, b, a + b, a + Tb, \dots, T^{N-1}b\} \tag{18}$$

where $T^i a$ denotes the operator that produces the sequence whose k-th element is given by a_{k+i}. It should be noted that Gold codes are generated via Linear Feedback Shift Registers (LFSR) as their structure undertakes two binary polynomials as it is illustrated in figure 10.

Balanced Gold Codes

A balanced code is a code in which the number of “ones” exceeds the number of “zeros” by one. This kind of codes have desirable spectral properties, however not all Gold codes are balanced codes. In order to obtain a family of balanced Gold codes, the following procedure [14] must be followed:

- First select a preferred pair of m-sequences *a* and *b* of length $N = 2^n - 1$.
- The initial conditions for shift register 2 are obtained by long division of the ratio $g(x)/f(x)$,where $f(x)$ is the characteristic polynomial of sequence b and $g(x)$ is defined as: $g(x) = f(x) + \frac{d[xf(x)]}{dx}$.
- The initial conditions for shift register 1 correspond to all ones.
- The set of Gold codes is formed by modulo-2 addition of the two registers, 1 and 2.

Designing a Balanced Gold Code

1- Select the first polynomial
   a. $x^{10} + x^3 + 1 \rightarrow 010000001001 \rightarrow 2011$
2- Select the second polynomial
   a. $K = 2 \rightarrow q = 2^k + 1 = 5 \rightarrow \text{greatest common divisor}(10,2) = 2$
   b. $Find\ in\ Annex\ C\ of\ [15] the\ \text{“}decimation\ of\ m - sequence\text{”}\ for\ b = a[5]$
   c. $b = a[5] = x^{10} + x^8 + x^3 + x^2 + 1 \rightarrow 010100001101 \rightarrow 2415$
3- As we want balanced codes we have to obtain the characteristic phase of the sequence b
   a. $g(x) = f(x) + \frac{d[xf(x)]}{dx} = x^3$
   b. $G(x) = longDivision({x^3}/{x^{10} + x^8 + x^3 + x^2 + 1}) \rightarrow x^7 + x^5 + 1$
4- Initial registers:
   a. $Init_a = 1111111110$

b. $Init_b = 0010100001$

Figure 10 give us the schema for the balanced Gold

5- From the sequences a and b we can obtain the family as:

$$G(a,b) = \{a, b, a+b, a+Tb, \ldots, T^{N-1}b\}$$

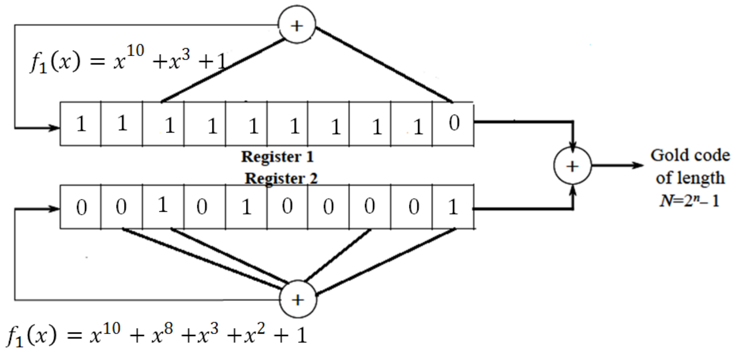

Figure 10 Balanced Gold Code Candidate for the New Acquisition-Aiding Signal

Large Kasami Codes

The large Kasami codes [14], like the Gold codes, are a set of periodic sequences with good correlation properties. Large Kasami codes have a code period of $N = 2^n - 1$ chips under the condition of $d(n,4) = 2$. Moreover the family size is equal to $(N+2)\sqrt{N+1}$. In order to construct the large Kasami codes, a small set of Kasami codes [14] is required. Small Kasami codes, as well as *No* codes, have the most outperforming correlation properties for a code length of 1023 chips, however the family size is just $\sqrt{N+1} = 32$ codes, which is not large enough to cope with all of the satellites of one GNSS constellation.

Following theorem 4 [14], and for the specific code length of $N = 1023$, a *preferred pair of m-sequences* a and c are defined. In addition, let $b = a[s(n)]$ denotes an m-sequence of period $2^{(\frac{n}{2})} - 1$ generated by the characteristic polynomial of degree n/2, b is the decimation sequence of a defined by:

$$b = a\left[2^{(\frac{n}{2})} + 1\right] = a[33] \tag{19}$$

The set of sequences defined by $K_L(a)$ is then the Large set Kasami sequences:

$$K_L(a) = G(a,c) \cup \left[\bigcup_{i=0}^{2^{(\frac{n}{2})}-1} \{T^i b + G(a,c)\}\right] \tag{20}$$

The family size is equal to $(N+2)\sqrt{N+1}$=32800 codes, whereof the most outperforming in terms of correlation terms are selected.

Design of Large Kasami Codes

1- Select the first Polynomial
   a. $x^{10} + x^3 + 1 \rightarrow 010000001001 \rightarrow 2011$
2- Select the second Polynomial
   a. $K = 2 \rightarrow q = 2^k + 1 = 5 \rightarrow \text{greatest common divisor}(10,2) = 2$
   b. $Find\ in\ Annex\ C\ of\ [15] the\ \text{“}decimation\ of\ m - sequence\text{”}\ for\ c = a[5]$
   c. $c = a[5] = x^{10} + x^8 + x^3 + x^2 + 1 \rightarrow 010100001101 \rightarrow 2415$
3- Select the third Polynomial
   a. $b = \left[2^{(\frac{n}{2})} + 1\right] = a[33]$
   b. $Find\ in\ Annex\ C\ of\ [15] the\ \text{“}decimation\ of\ m - sequence\text{”}\ for\ b = a[33]$
   c. $c = a[33] = x^5 + x^4 + x^3 + x^2 + 1 \rightarrow 000000111101 \rightarrow 0075$
4- From the sequences a, b and c we can obtain the family as:

a. $K_L(a) = G(a,c) \cup [\bigcup_{i=0}^{2^{(\frac{n}{2})}-1}\{T^i b + G(a,c)\}]$

Random Sequences

A method to create a set of spreading codes with good correlation properties is provided in [6]. The method comprises building an initial set of random bits patterns, where each bits pattern represents a potential spreading code, and provides enhanced performances compared to the initial set of bits, the ultimate goal being to select an optimized final set of spreading codes. A cost function must be defined in order to determine if the current iteration provides a better solution than the precedent one. As a new Acquisition-Aiding signal is the design goal, a cost function which evaluates the unwanted correlation peaks (those which increase the acquisition error probability) is hence proposed [6]. Therefore any correlation value which exceeds the Welch bound is considered as a degradation of the system. Equation 21 provides the cost function.

$$F_i = \sum_{\substack{l=1 \\ ACF^e(l)>\Phi_{min}}}^{N-1} (ACF^e(l) - \Phi_{min})^2 + \sum_{j\neq i} \sum_{\substack{l=1 \\ {CC_j}^e(l)>\Phi_{min}}}^{N-1} ({CC_j}^e(l) - \Phi_{min})^2 \quad (21)$$

Each algorithm iteration comprises two steps: a chip flip within the spreading code and the evaluation of the cost function. If the chip flip minimizes the cost function regarding the previous iteration, the chip flip is accepted; otherwise the chip flip is discarded. The flow diagram of the algorithm is illustrated in figure 11.

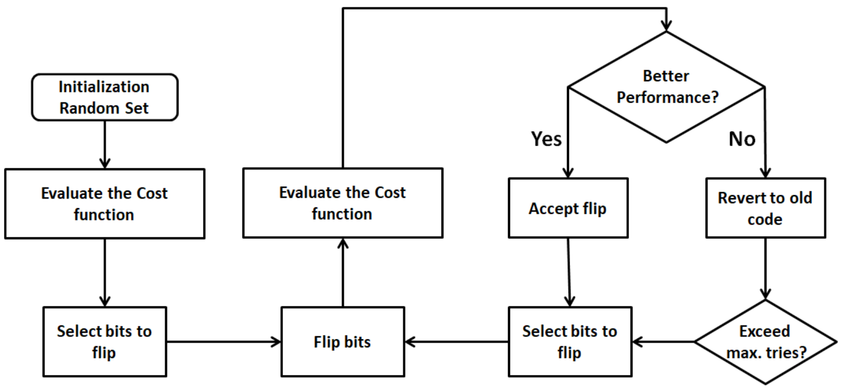

Figure 11 Diagram Flow for Optimization or Random Sequence

It is well known that both balanced and minimum ACF side-lobe properties are desired spreading codes characteristics. These properties can be set as initial requirements for the initial set of codes. However, after flipping some of the bits, those qualities could not be kept. In order to guarantee those desired properties, two precursor conditions [6] are imposed on the flipping bit step. The first one is the *balanced invariance condition* [6] where bits are always flipped in pairs, i.e., one bit with null value and one bit with value 1 are flipped to ensure that the code remains balanced. The second condition is to *minimize the ACF side-lobe.* This property can be ensured by following equation 22.

$$a_{k-1} + a_{k+1} = a_{j-1} + a_{j+1} \quad (22)$$

where a_k and a_j are the flipping bits.

The initial solution could affect both the time convergence and the final solution performance. In order to select an initial feasible solution, the balanced Gold codes or the balanced large Kasami codes, under the minimum ACF side lobe condition are proposed as initial codes.

V SPREADING CODES ASSESSMENT

In this section, five families of spreading codes are compared:

- Gold codes,
- Large Kasami codes,
- Random codes with a random array as an initial solution,
- Random codes with Gold codes as initial solution and
- Random codes with large Kasami codes as initial solution.

Those families are compared under the criteria defined in section III. All codes are balanced and have the minimum ACF side-lobes. The size of the subset of codes used to evaluate the performance is 100 codes. To select the hundred codes Gold family and the hundred codes Kasami family, the best 100 codes under (21) have been considered. In the case of Random Codes families, the optimization process iterates a fixed number of iterations equal to 20000, which is considered large enough for the convergence of the optimization process. Table 6 summarizes the different criteria values for the 5 families of codes. From table 6, it can be gathered that the hence defined criteria are not of the same order of magnitude and should all be normalized in order to make a fair comparison between them. This is the main justification for computing a relative weight cost function (17). It is also remarkable that random codes families values are very close for the 5 criteria, with better $\mathrm{AMEWSD}^{\mathrm{MP}}$ and $\mathrm{AMEWSD}^{\mathrm{CT}}$ values if we compare with the Gold and Kasami families. This can be explained by the fact that the minimization problem computed in the random codes generator process consists in minimizing both the $\mathrm{AMEWSD}^{\mathrm{MP}}$ and $\mathrm{AMEWSD}^{\mathrm{CT}}$ criteria.

	Gold Codes	*Large Kasami Codes*	*Random codes*	*Random codes Init. Gold Codes*	*Random codes Init. Kasami Codes*
$AMEWSD^{MP}$	0.09550	0.0911	0.0881	0.08840	0.08881
$AMEWSD^{CT}$	0.09629	0.09127	0.09022	0.09035	0.09018
AMF^{MP}	0.00096	0.00096	0.00094	0.00099	0.00094
AMF^{CT}	0.98985	0.9903	0.98946	0.98944	0.9894
$AELW$	19.5320	19.5670	19.2296	19.2905	19.25164

Table 6 Selection Criteria for 5 Families of Spreading Codes

Table 7 illustrates the weighted relative criteria expressed in (%) for the 5 families of spreading codes. In this table, the results of the cost function are also illustrated as well as the ranking position between the 5 families. Furthermore, a weighting criterion with a uniform weight vector, $Weight = [0.2, 0.2, 0.2, 0.2, 0.2]$, is applied. Thanks to the cost function, an objective criterion can be defined to obtain the spreading codes family ranking. From the ranking row, random codes family obtains the best cost function value and consequently is considered as the best set of codes among the five families. Figure 12 illustrates the weight cost function results of table 7.

Figure 13 illustrates the weighted criteria and the weight cost function solution for a weighting criterion with a weight vector equal to $Weight = [0.35, 0.35, 0.1, 0.1, 0.1]$. In this example, more importance is given to the acquisition criteria and consequently those families of codes with better performances on $\mathrm{AMEWSD}^{\mathrm{MP}}$ and $\mathrm{AMEWSD}^{\mathrm{CT}}$ improve their relative cost function value.

	Gold Codes	*Large Kasami Codes*	*Random codes*	*Random codes Init. Gold Codes*	*Random codes Init. Kasami Codes*
$AMEWSD^{MP}$*(%)*	0.0565	0.0087	-0.0258	-0.02198	-0.0174
$AMEWSD^{CT}$*(%)*	0.0504	-0.0042	-0.0157	-0.01432	-0.0161
AMF^{MP}*(%)*	-0.0017	0.0031	-0.0186	0.03313	-0.0158
AMF^{CT}*(%)*	0.00015	0.00063	-0.00024	-0.00026	-0.00027
$AELW$*(%)*	0.0081	0.0099	-0.0074	-0.0043	-0.0063
Cost Function	2.2721	0.3651	-1.3599	-0.1551	-1.1221
Ranking	5	4	1	3	2

Table 7 Weighted Relative Criteria for 5 Families, $\boldsymbol{Weight = [0.2, 0.2, 0.2, 0.2, 0.2]}$

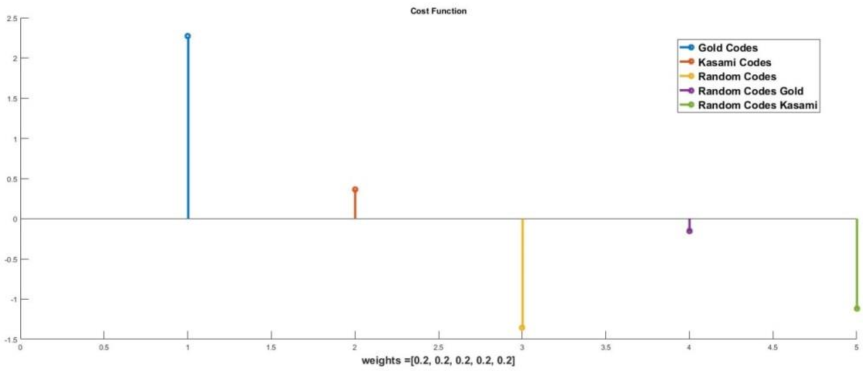

Figure 12 Weighted Cost Function Results for 5 Families, $\boldsymbol{Weight} = [\mathbf{0.2}, \mathbf{0.2}, \mathbf{0.2}, \mathbf{0.2}, \mathbf{0.2}]$

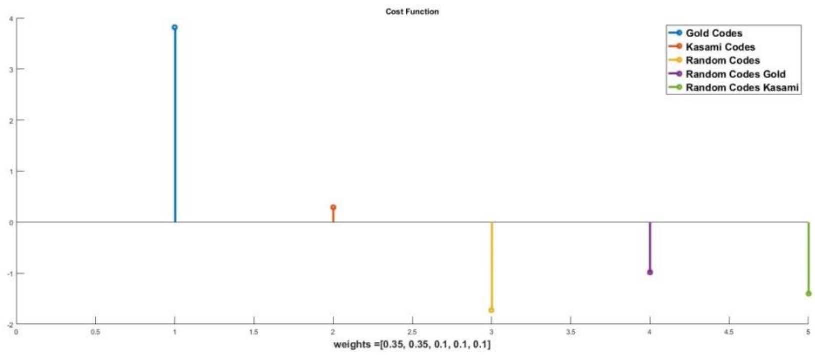

Figure 13 Weighted Cost Function Results for 5 Families, $\boldsymbol{Weight} = [\mathbf{0.35}, \mathbf{0.35}, \mathbf{0.1}, \mathbf{0.1}, \mathbf{0.1}]$

From figures above, it can be verified that the performance of the random codes families with an initial solution from Gold or Kasami codes are worse than the random code family with a random initial array. This situation can happen when the number of iterations is large, as is the case here (20000 iterations).

CONCLUSION

This paper has described the methodology followed to study two critical issues for the development of a new Acquisition-Adding signal for the future GNSS Galileo system. A new spreading modulation compatible with the current GNSS systems as well as a new spreading codes family enabling the reduction of the false acquisition probability under hostile environments have been subject of our study.

Several criteria such as the interference compatibility, correlation properties, multipath effect, ranging performance or anti-jamming capability have been evaluated in order to select the new spreading modulation. Among all these properties, the Radio Frequency Compatibility evaluated by the Spectral Separation Coefficients establishes an acceptability criterion due to an interference compatibility requirement. Furthermore, to ease the acquisition process, one must seek for a high first to secondary peak-to-peak ratio in the autocorrelation function. Simulation results show that the BCS[-1 -1 -1 1 -1](1) spreading modulation is considered as the most interesting solution.

Selection criteria based on the auto- and cross-correlation as well as the Doppler offset have been taken into account for selecting the new spreading codes family. Those criteria describe both acquisition and tracking modes as well as the multipath and narrow band interference effects. In order to assess all the criteria, a relative weighed cost function has been evaluated. Several families have been compared with the cost function: the Gold and large Kasami families, which have been designed following a mathematical model and a random codes family which is computed based on a cost function minimization process. Simulation results show how the random code family outperforms the remaining candidates in terms of acquisition process by exhibiting the lowest cost function among all the candidate codes families.

Future works will investigate other aspects such as channel coding or the data message structure in order to develop the new Acquisition-Adding signal for the future GNSS Galileo System.

ACKNOWLEDGMENTS
This work is funded by the French Space Agency, CNES, and Thales Alenia Space.

REFERENCES

[1] Paonni, M., Bavaro, M., "On the Design of a GNSS Acquisition Aiding Signal," Proceedings of the 26th International Technical Meeting of The Satellite Division of the Institute of Navigation (ION GNSS+ 2013), Nashville, TN, September 2013, pp. 1445-1456.

[2] ITU-R M.1831-1 “A coordination methodology for radionavigation-satellite service inter-system interference estimation”.

[3] F. Soualle, M. Soellner, S. Wallner, J. Avila-Rodriguez, G. Hein, B. Barnes, T. Pratt, L. Ries, J. Winkel, C. Lemenager, and P. Erhard. “Spreading Code Selection Criteria for the future GNSS Galileo”

[4] Hegarty, Chris, Betz, John W., Saidi, Ali, "Binary Coded Symbol Modulations for GNSS," Proceedings of the 60th Annual Meeting of The Institute of Navigation (2004), Dayton, OH, June 2004, pp. 56-64.

[5] Betz, John W., "BINARY OFFSET CARRIER MODULATIONS FOR RADIONAVIGATION", NAVIGATION, Journal of The Institute of Navigation, Vol. 48, No. 4, Winter 2001-2002, pp. 227-246.

[6] Jon Olafur Winkel, US 2008/0246655 A1, “SPREADING CODES FOR A SATELLITE NAVIGATION SYSTEM”.

[7] Oppenheim, Alan V, Alan S. Willsky, and Ian T. Young. Signals and Systems. Englewood Cliffs, N.J: Prentice-Hall, 1983.

[8] Elliott D. Kaplan. Understanding GPS: Principles and Applications. Boston: Artech House, 1996.

[9] Irsigler, Markus, Avila-Rodriguez, Jose Angel, Hein, Guenter W., "Criteria for GNSS Multipath Performance Assessment," Proceedings of the 18th International Technical Meeting of the Satellite Division of The Institute of Navigation (ION GNSS 2005), Long Beach, CA, September 2005, pp. 2166-2177.

[10] Liu, X.; Liang, M.; Morton, Y.; Closas, P.; Zhang, T.; Hong, Z. Performance evaluation of MSK and OFDM modulations for future GNSS signals. GPS Solut. 2014, 18, 163–175.

[11] D. V. Sarwate M. B. Pursley "Crosscorrelation properties of Pseudorandom and related sequences" Proceedings of the IEEE vol. 68 no. 5 pp. 593-618 May 1980.

[12] M. B. Pursley H. F. A. Roefs "Numerical evaluation of correlation parameters for optimal phases of binary shift register sequences" IEEE Trans. Commun vol. COM-27 no. 10 Oct. 1979.

[13] S. Wallner and J.-A. Ávila-Rodríguez. “Codes: The PRN Family Grows Again” Inside GNSS, Volume 1, September, 2011

[14] “Spread Spectrum Systems for GNSS and Wireless Communications”, Chapter 2, Jack K. Holmes

[15] “Error Correcting Codes” W. Wesley Peterson, MIT Press (1970)

[16] Betz, John W., "Effect of Narrowband Interference on GPS Code Tracking Accuracy," Proceedings of the 2000 National Technical Meeting of The Institute of Navigation, Anaheim, CA, January 2000, pp. 16-27.

[17] R. Xue, Y. Sun, and D. Zhao, “CPM signals for satellite navigation in the S and C bands,” Sensors, vol. 15, no. 6, pp. 13184–13200, 2015.

[18] Rui Xue, Qing-ming Cao, and Qiang Wei, “A Flexible Modulation Scheme Design for C-Band GNSS Signals,” Mathematical Problems in Engineering, vol. 2015, Article ID 165097, 8 pages, 2015. doi:10.1155/2015/165097.